Supplementary Information

Structural and Functional Bases for Broad-Spectrum Neutralization of Avian and Human Influenza A Viruses

Jianhua Sui [1], William C. Hwang [2], Sandra Perez [3], Ge Wei [2], Daniel Aird [1], Li-mei Chen [3], Eugenio Santelli [2], Boguslaw Stec [2], Greg Cadwell [2], Maryam Ali [1], Hongquan Wan [3], Akikazu Murakami [1], Anuradha Yammanuru [1], Thomas Han [1], Nancy J. Cox[3], Laurie A. Bankston [2], Ruben O. Donis [3], Robert C. Liddington [2] and Wayne A. Marasco [1]

[1]Department of Cancer Immunology & AIDS, Dana-Farber Cancer Institute; Department of Medicine, Harvard Medical School, 44 Binney St. JFB 826, Boston, MA 02115, USA

[2]Infectious and Inflammatory Disease Center, Burnham Institute for Medical Research, 10901 North Torrey Pines Road, La Jolla, CA 92037, USA.

[3]Influenza Division, Centers for Disease Control and Prevention, National Center for Immunization and Respiratory Diseases, 1600 Clifton Road - Mail Stop G-16, Atlanta, GA 30333, USA.

Nature Structural & Molecular Biology: doi:10.1038/nsmb.1566

Supplementary Fig. 1

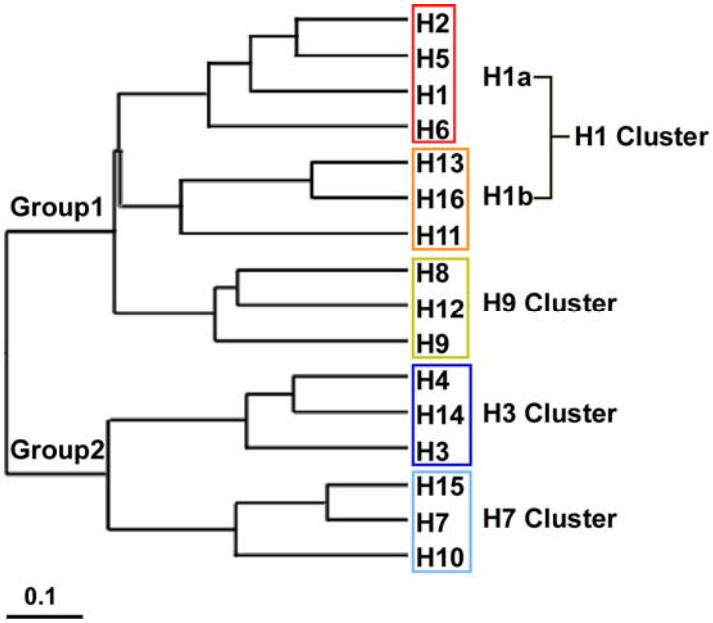

Fig. S1. Phylogenetic relationships among HA subtypes. Phylogenetic tree of the 16 HA subtypes of influenza A viruses based on amino-acid sequences. Four clusters of HA subtypes are shaded in different colors. The sequences used for analysis were:
H1 (A/South Carolina/1/1918),H2 (A/Japan/305/1957),
H3 (A/Aichi/2/1968), H4 (A/duck/Czechoslovakia/56),
H5 (A/VietNam1203/2004), H6 (A/chicken/California/431/00),
H7 (A/Netherland/219/03), H8 (A/turkey/Ontario/6118/68),
H9 (A/swine/HK/9/98), H10 (A/chicken/Germany/N49),
H11 (A/duck/England/56), H12 (A/duck/Alberta/60/76),
H13 (A/gull/Maryland/704/77), H14 (A/mallard/Astrakhan/263/1982),
H15 (A/shearwater/West Australia/2576/79)
and H16 (A/black-headed gull/Sweden/2/99).

Supplementary Fig. 2

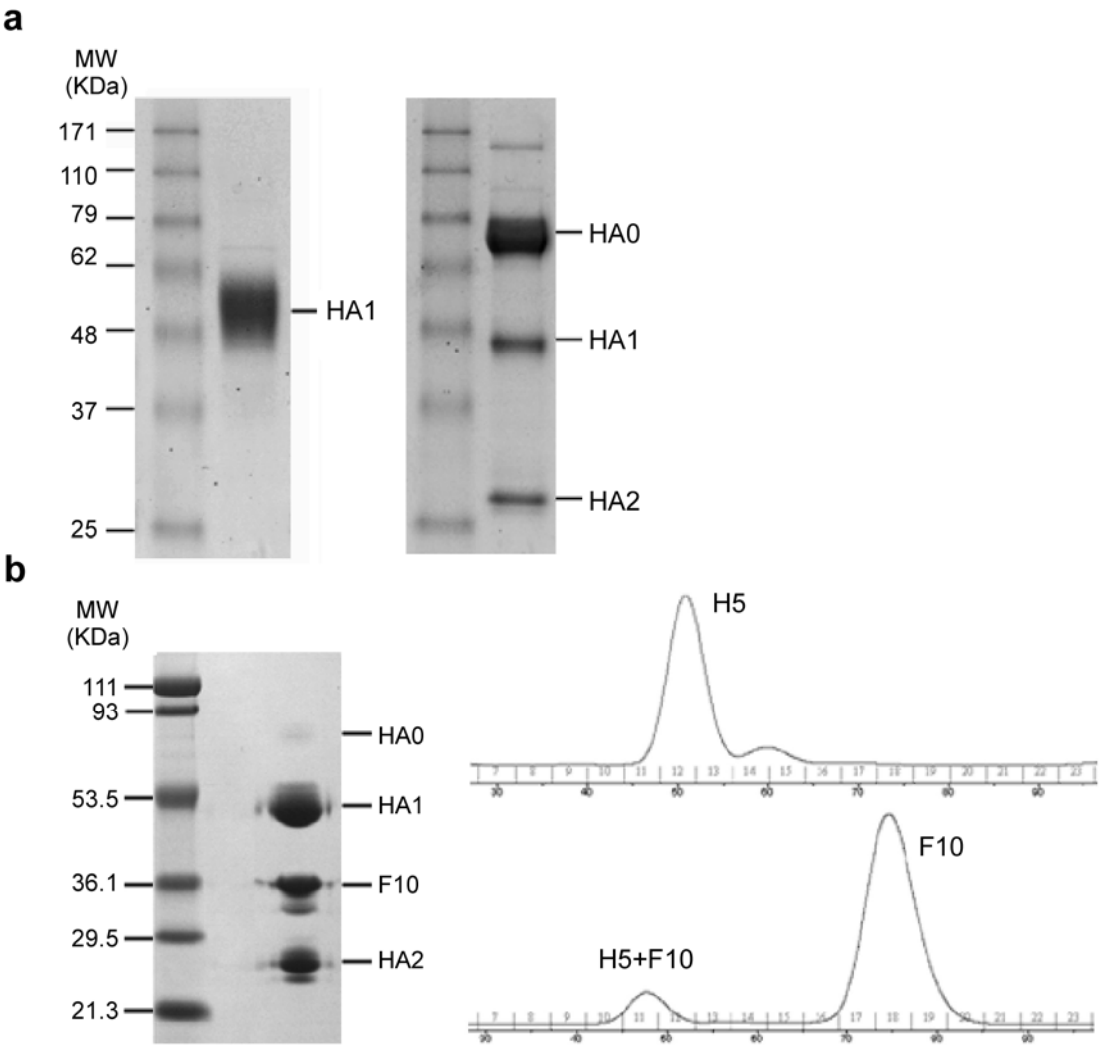

Fig. S2. SDS-PAGE and gel filtration analysis of HA proteins. (a) HA1-specific antibody 2A was obtained from a separate HA1-targeted selection against the HA1 (residues 11-325) fragment of H5-TH04 (left panel). H5 HA (H5-VN04 strain) used for library selection is shown in the right panel (the majority is uncleaved HA0). **(b)** H5-VN04 (H5) and scFv F10 complex. HA0 was fully cleaved into HA1 and HA2 by co-expression with furin (left panel). Complexes were formed by first mixing H5 and F10 at a molar ratio of 1:10, and then purified by gel filtration.

Supplementary Fig. 3

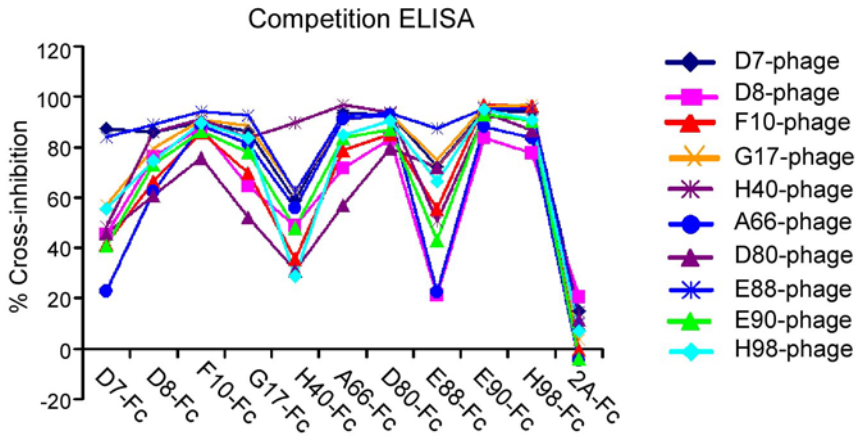

Fig. S3. Competition ELISA assay between soluble and phage-bound nAbs. All anti-H5 nAbs cross-competed, consistent with an overlapping epitope, while anti-HA1 ("2A-Fc") did not. 10^{12} pfu of anti-H5 phage-scFv-Fcs were mixed with 5 μg/mL of soluble nAbs and added to H5-VN04-coated plates, washed, and followed by HRP-anti-M13 to detect phage-bound H5**.**

Supplementary Fig.4

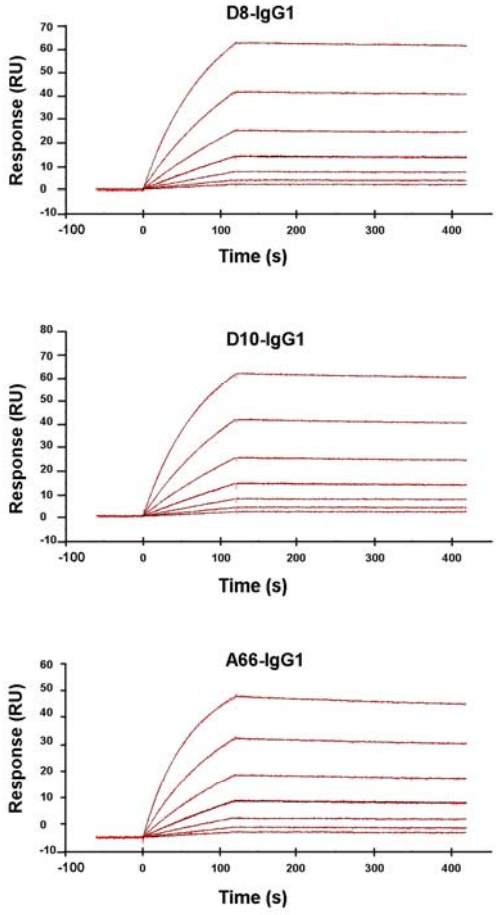

$$A + B \underset{kd}{\overset{ka}{\rightleftharpoons}} AB$$

	ka (M^{-1} s^{-1} x 10^5)	kd (s^{-1}x10^{-4})	K_D (pM)
D8-IgG1	5.98±0.08	0.88±0.11	148±19
F10-IgG1	6.52±0.92	0.84±0.19	130±28
A66-IgG1	7.75±0.63	1.80±0.31	233±47

Fig. S4. Kinetic and thermodynamic characterization of the binding of H5 HA to nAbs D8, F10 and A66-IgG1s. nAbs were captured on a CM4 chip via anti-human IgG1; trimeric H5 (H5-VN04) at various concentrations (20, 10, 5, 2.5, 2.5, 1.25, 0.625 nM) was injected over the chip surface. Binding kinetics were evaluated using a 1:1 Langmuir binding model. The recorded binding curves (with blank reference subtracted) and the calculated curves are closely superimposable. Each *ka, kd* and K_D value represents the mean and standard error of three experiments.

Supplementary Fig. 5

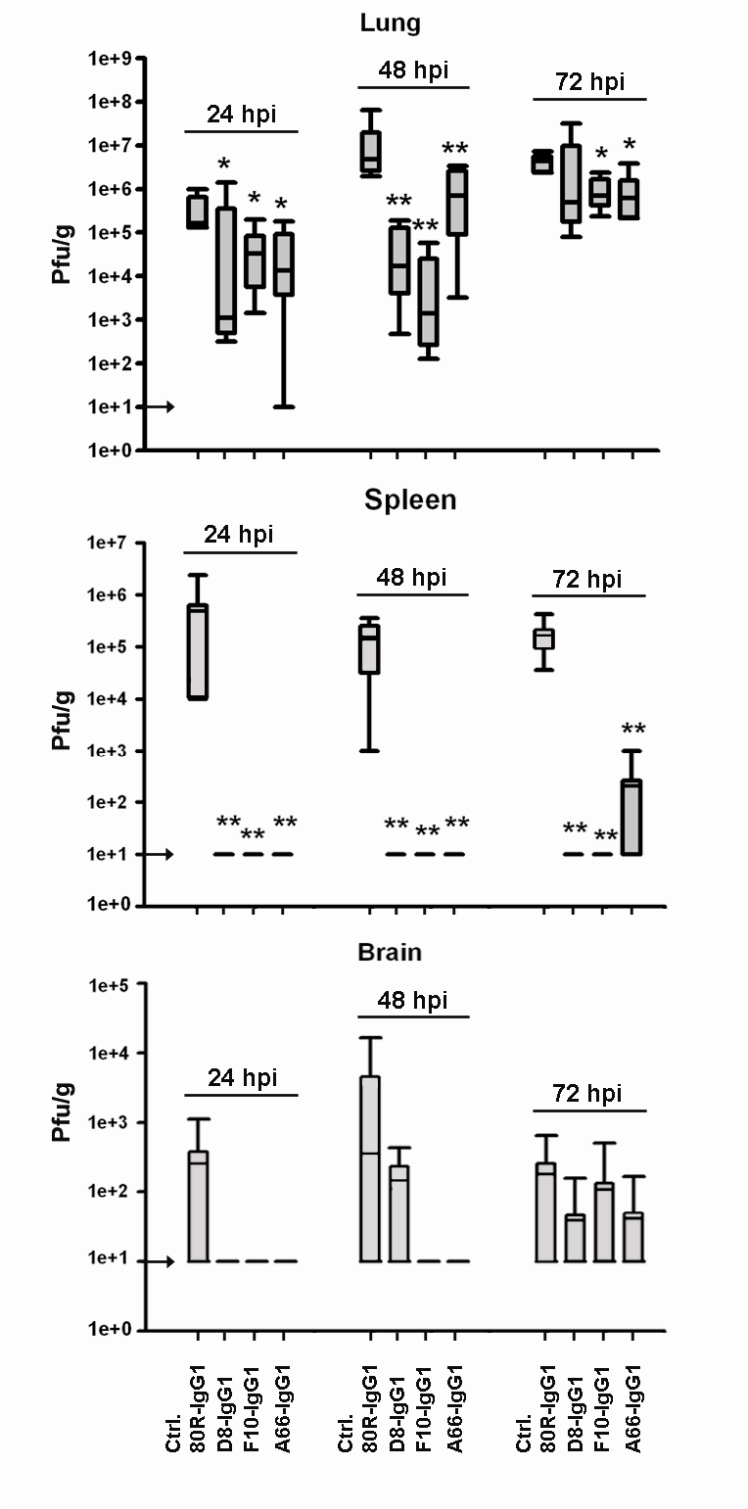

Fig. S5. Viral titers in lung, spleen and brain of mice treated with anti-H5 nAbs after H5-VN04 challenge. BALB/c mice (n=5) were treated by i.p. injection of 15 mg/kg of mAb at 24, 48 or 72 hrs after i.n. infection with 10 MLD_{50} of H5-VN04 as described in Fig 3 of the main text. Viral titers were determined at 96 hpi either in lungs, as an indicator of inhibition of local replication, or in spleen and brain, indicative of the systemic spread that is characteristic of H5N1 infection. The nAbs mediated a significant suppression of viral replication in lungs when given within 48 hours of challenge. Notably, two of the nAbs, D8 and F10, also showed significant antiviral effect when given at 72 hpi. The impact of nAb therapy on systemic spread was demonstrated by ≥ 1000-fold suppression of virus spread to the spleen even when the three nAbs were given within 72 hpi. Systemic virus spread to the brain was low in control animals, obscuring statistically significant effect of nAb treatment, but still showing a general pattern of suppression. Data are displayed in box-and-whiskers form in which the box extends from the 25^{th} to the 75^{th} percentile, with a horizontal line at the median. Whiskers above and below the box indicate the extreme values. Results of Student T-test statistic analysis are noted with a single star (*) for $p<0.05$, and double stars (**) for $p<0.01$. The arrows crossing the y-axis indicate the detection limit of the titration.

Supplementary Fig.6

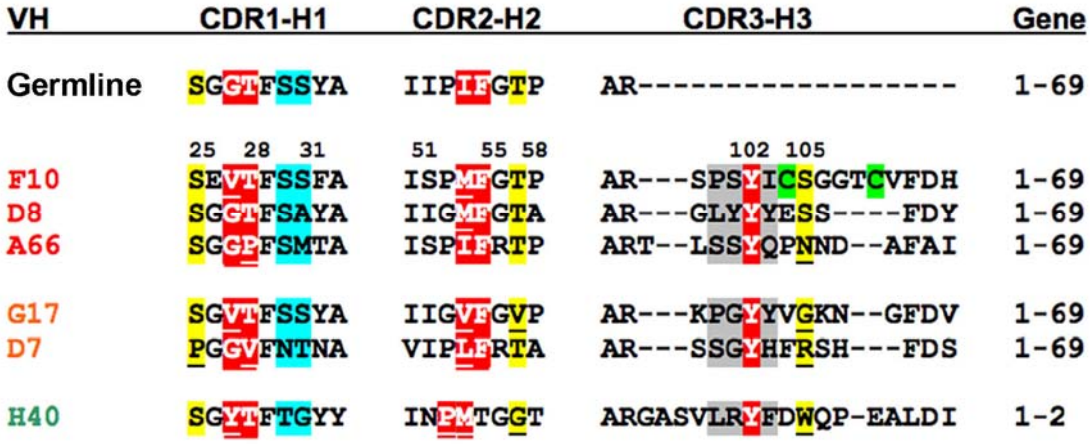

Fig. S6. Sequence conservation within CDR regions of the 6 distinct nAb VH genes. Five genes are derived from the same germline gene, IGHV1-69 ("1-69"), shown on the first line. The CDR3 loop is encoded by other genetic elements. The VL genes (Supplementary Table 1) are much more diverse since they do not contact H5. The 3 VH genes used to make IgG1s are labeled in red. Contact residues are highlighted in different colors based on their estimated contribution to binding: red (very favorable); yellow (favorable); blue (neutral); and gray (unfavorable). Residue differences from the consensus at favorable contacts are underlined. The G=>E mutation at position 26 of F10 induces a non-canonical conformation of H1; the others are predicted to have consensus loop structures. The H2 loop closely follows the consensus "type 2" structure defined by Chothia et al.[1]. The disulfide-bonding pair in the F10 H3 loop is highlighted in green. The H2 loop of the 1-2 gene is predicted to adopt a conformation ("type 3") different from 1-69, in which the highlighted proline and methionine are exposed at its tip. The correspondence of the tyrosine in H3 of H40 is also speculative.

Supplementary Fig. 7

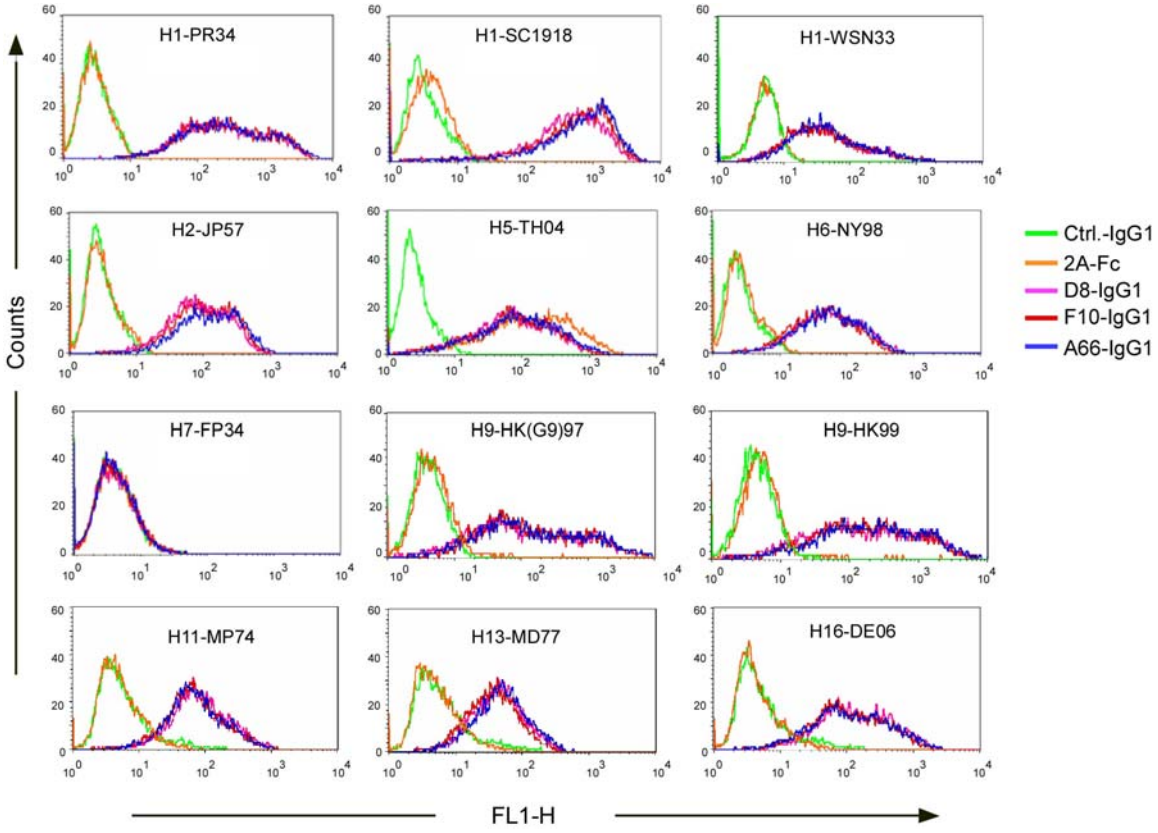

Fig. S7. NAbs bind to a broad range of Group 1 HA subtypes. FACS analysis of anti-H5 nAbs binding to H1, H2, H5, H6 (Cluster H1a), H11, H13 and H16 (Cluster H1b) and H9 (H9 Cluster). 293T cells were transiently transfected with different HA-expressing plasmids, and mAb binding to the cells was analyzed by FACS. H5-specific antibody 2A and 80R are negative control. Lack of binding to a Group 2 HA, H7, is also shown. Complete viral strain designations are: H7-FP34 (A/FPV/Rostock/34 (H7N1)), H13-MD77 (A/gull/MD/704/77 (H13N6)) and H16-DE06 (A/shorebird/DE/172/06 (H16N3)); and see Fig. 6 (main text) for others.

Supplementary Fig. 8

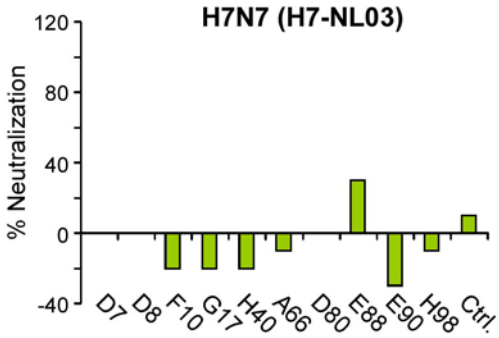

Fig. S8. Anti-H5 nAbs do not neutralize H7N7 influenza virus. 10 H5-selected scFv-Fc Abs were tested for neutralizing activity against H7-NL03 (A/Netherlands/219/2003 (H7N7)) virus in a plaque reduction assay. These results are representative of two independent experiments.

Supplementary Fig. 9

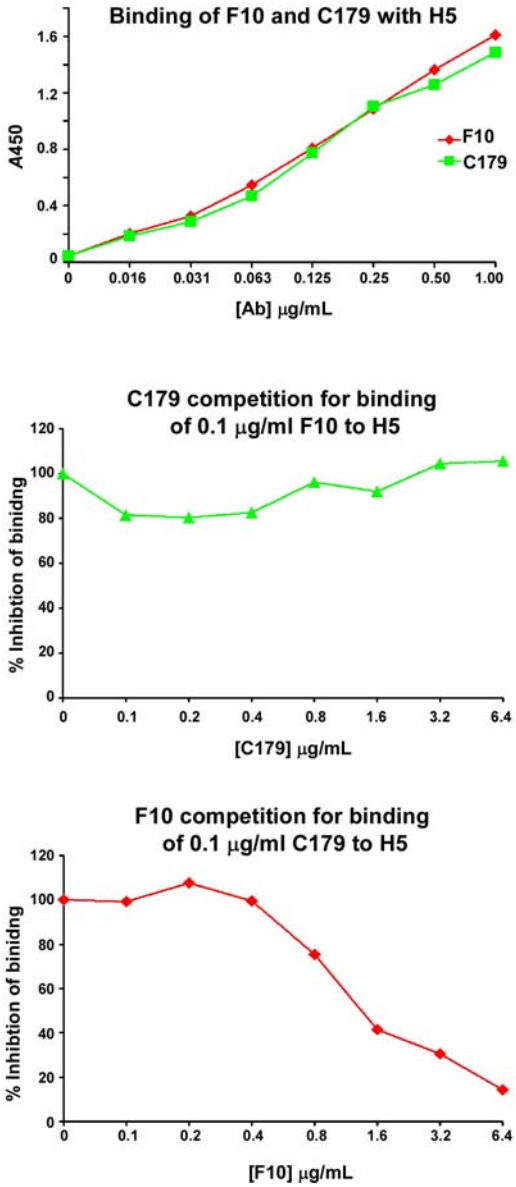

Fig. S9. Binding of F10 or C179 to H5 and cross-competition ELISA for F10 and C179. 0.2 μg of H5 HA proteins were coated onto 96-well ELISA plates for these experiments. Top panel: binding of F10 or C179 to H5 was tested with 2-fold serial dilutions of antibody. Middle and bottom panels: F10 and C179 cross-competition ELISAs. 0.1 μg mL^{-1} C179 or F10 were mixed with different concentrations of F10 or C179.

Supplementary Table 1. Amino acid sequences of variable regions of anti-H5 mAbs

VH	FR1	CDR1	FR2	CDR2	FR3		CDR3	FR4	V GENE
Cons.	KKPGSSVKVSCKAS	GGTFSSYA	ISWVRQAPGQGLEWMGG	IIPMFGTP	NYAQKFQGRVTITADESTSTAYMELSSLRSEDTAVYYC	AR		WGQGTL	
IGHV1-69	....	.GT.SS..	....	...IF.TA	....	..			1-69*01
F10/E90	...........TSS	EVT.SSF.	..............L..	.S.MF.T.	...............Q..R....D.R............	..	---SPSYICSGGTCVFDH	......	1-69*01
D8/D80	....	.GT.SA..	FT...............	..GMF.TA	................L...........T.....L...	..	---GLYYYESS----FDY	......	1-69*01
A66/E88	....	.GP.SMT.	FT.L.............	.S.IFRT.	K.................N..N...T..K.........	..	--TLSSYQPNND--AFAI	.....M	1-69*01
G17	....A.......T.	.VT.SS..	....	..GVF.V.	K..............KP...V....N...A........	..	---EPGYYVGKN--GFDV	.....M	1-69*06
D7/H98	.............P	.GI.NTN.	F.............V..	V..LFRTA	S...NV............N......T....A.......	..	---SSGYHFRSH---FDS	..L...	1-69*01
H40	R...A.........	.YT.TG.Y	.H..............W	.NPMT.GT	.......VW..M.R.T.IN.....VTR.T.D.......	..	GASVLRYFDWQP-EALDI	..L..T	1-2
IGHV1-2	....A.........	.YT.TG.Y	MH..............R	.NPNS.GT	...........S.R.T.I........R......V....	..			

VL	FR1	CDR1	FR2	CDR2	FR3	CDR3	FR4	GENE
Cons.	QPVLTQPPS-ASGSPGQRVTISCTGS		VAWYQQKPGQAPKLLIY		DRPSGIPDRFSGSR--SGTTASLTISGLQPEDEADYYC		FGGGTKLTVL	
D7Vλ	NFM....H.-V.A...KT........	SGNIAANY	.Q....R..S..TTV..	EDD	R....V.......IDR.SNS........KT........	QTYDTNNHAV	.....H....	LV6-57
D8Vλ	.S.......-.......S.......T	SSDVGGYNS	.S....H..K....M..	EVT	K....V.....A.K--..N.....V....A......F.	CSYAGHSAYV	..T...V...	VL2-11
F10Vλ	..G......-V.KGLR.TA.LT...N	SNNVGNQG	A..L..HQ.HP....S.	RNN	......SE...A..--..N......T............	STWDSSLSAVV	....	LV10-54
G17Vλ	SYE......-V.KGLR.TAILT...D	SNNVGHQG	T..L..HQ.HP....S.	RNG	N.....SE...A..--..N......I............	SVWDSSLSAWV	....	LV10-54
H40Vλ	.........-V.VA...TAS.P.G.N	NIGGYS--	.H..........L.V..	DDK	.......E....AN--..S..T....RVEAG..G....	QVWDSGNDRPL	....	VL3-21
A66Vκ	EI....S.ATL.L...E.A.L..RA.	QSVSSY--	L...........R....	DAS	N.AT...A.....G--...DFT....R.E...F.V.F.	QQYGSSPQ---	..Q..R.EIK	KV3-20
D80Vκ	EI....S.GTL.L...E.A.L..RA.	QSLSSKY-	L...........R....	GAS	S.AT.........G--...DFT....R.E...F.V.S.	QQYDGVPRT--	..Q..TVEIK	KV3-20
E88Vλ	L........-...T......I..S..	SSNIGSNT	.N....L..T.......	SNN	Q....V........--...S...A.I..R.........	QSYDSRLSASL	..T..TV...	LV1-44
E90Vκ	DIQM..S..SL.A.V.D....T.RA.	QSISSY--	LN.......K.......	AAS	SLQR.V.S.....G--...DFT....S.....F.V.Y.	QQYDSSPYT--	..Q...VEIK	KV1-39
H98Vλ	SYE......-...KH........S.G	TSNIGRNH	.N....L..T.......	SNE	Q....V.......K--...S...AV....S........	ASWDDNLSGWV	....	LV1-44

Framework regions 1-4 (FR1-4) and complementarity-determining regions 1-3 (CDR1-3) for VH and VL are shown. FR, CDR and gene names are defined using the IMGT database. For VH, the first 11 residues of FR1 (QVQLVQSGAEV) and last 5 residues of FR4 (VTVSS) are invariant and not shown. Dots denote identity with the consensus sequence, hyphens denote gaps. Six different VH and 10 different VL genes were found. 5 out of the 6 VHs belong to one gene family, IGHV1-69 (01 or 06 allele). H40 (colored in blue) uses IGHV1-2 germline gene. The VL genes are much more diverse than the VH genes, consistent with the lack of significant contacts observed between F10 and H5; three out of the 10 VL are κ chain. The 3 VH chains that were used to make IgG1s are colored red. H5 contact residues of F10 observed in the crystal structure are highlighted, along with corresponding residues in other VHs, in cyan (critical residues as defined by FastContact energy calculations) and grey (other contacts < 4.5 Å). Gln74 (important in stabilizing the CDR1 and CDR2 loop conformations) in FR3 is highlighted in green. The H2 loop of H40 is predicted to have a different conformation (see Fig. S6) with different residues at its tip. The residue at position 72 (magenta) largely determines the conformation of the H2 loop (Ala for “type 2” and Arg for “type 3”).

Table S2. Contact residues at the H5-F10 interface

F10	FR-H1	CDR-H1				CDR-H2			CDR-H3				
	Ser25	Val27	Thr28	Ser30	Ser31	Met54	Fhe55	Thr57	Pro100	Ser101	Tyr102	Ile103	Ser105
HA1	Ser291	Ser291 Met292		Gln40		His38	His18 His38						
HA2		Ile56	Trp49 Val52 Asn53		Ile45 Thr49	Trp21 Ile45	Val18 Asp19 Gly20 Trp21	Val18	Gln42	Gln42	Asp19 Lys38 Thr41 Gln42 Ile45	Asp19 Lys38	Lys38

H5-F10 contact residues defined by interatomic distances < 4 Å. The color scheme indicates contributions to the binding energy: very favorable (red); favorable (orange); neutral (blue) and unfavorable (black). For F10, the overall contribution for each residue is shown; for H5, the strength of individual interactions is indicated.

Supplementary Table 3. Sequence comparison of F10 epitope among 16 HA subtypes.

Group	Cluster	Subtype	# Full-length sequence	# Unique sequence	HA1						HA2												
					17	18	38	40	291	292	18	19	20	21	38	41	42	45	49	52	53	56	111
Group 1	H1a	H2	100	95	Y	H	H	(Q,E)/K (18)/77	T	(M)/L (1)/95	(I)/V (20)/75	D	G	W	K	T	Q	(F,V)/I (39)/56	T	(I)/V (1)/94	N	I	H
		H5	1620	1178	(S,T,F)/Y (4)/1174	(Y,M)/H (2)/1176	(Q,Y)/H (4)/1174	(K)/Q (2)/1176	(I,N,T,R)/S (6)/1172	(K,L,I)/M (24)/1154	(I)/V (6)/1172	(N,H,Y,X)/D (5)/1173	G	(R)/W (1)/1177	(Q,R,N)/K (23)/1155	(S)/T (3)/1175	P/Q (1)/1177	(M,L,T)/I (8)/1170	(I)/T (1)/1177	V	N	(F)/ V (1)/1177	H
		H1	1211	701	Y	H	H	(I)V (2)/699	(S)/N 16(685)	(F)/L (1)/700	(I,M)/V (131,6)/546	D	G	W	(K,R,L)/Q (60)/641	T	Q	(V)/I (2)/699	(S,N,X)/T (19)/682	(M,I)/V (2)/699	N	(V)/I (1)/700	H
		H6	278	230	Y	H	H	V	(I)/N (1)/229	(R)/K (4)/226	(V)/I (43)/187	D	G	(R)/W (1)/229	(R)/K (102)/128	T	Q	(V)/I (78)/152	(I)/T (1)/229	(I)/V (3)/227	N	I	H
	H1b	H13	16	16	Y	L	S	(V)/I (6)/10	N	(R)/K (8)/8	I	N	G	W	K	T	Q	I	T	V	N	I	H
		H16	8	6	Y	L	S	(I)/V (2)/6	N	K	I	N	G	W	K	T	Q	I	T	V	N	I	H
		H11	64	64	Y	L	S	(I)/V (1)/64	(T)/S (1)/63	(K)/R (23)/41	(L)/I (1)/63	N	G	W	(R)/K (5)/59	T	Q	(V)/I (3)/61	(I)/T (1)/63	V	N	(I,A)/V (17)/47	H
	H9	H8	10	10	Y	Q	Q	M	S	K	I	D	G	W	Q	T	Q	I	T	(I)/V (1)/9	N	I	H
		H12	19	18	Y	Q	Q	E	S	K	V	A	G	W	R	T	Q	I	Q	L	N	I	H
		H9	252	234	(H)/Y (33)/201	(L)/Q (1)/233	(D)/H (1)/233	(R,E)/K (5)/229	(I)/T (1)/233	(M)/L (1)/233	V	(S)/A (1)/233	G	(G)/W (1)/233	(K,G)/R (14)/220	T	Q	(V,F,M,R)/I (43)/191	(I)/T (1)/233	V	(S,T,D)/N (3)/231	(I)/V (55)/179	(C)/H 1/233
Group 2	H3	H4	105	90	H	H	(A)T (1)/89	(R)Q (1)/89	(A,I,S,N)/T (10)/82	K	I	D	G	(G)/W (1)/91	L	T	Q	I	(N)/T (1)/89	L	N	I	(A)/T (2)/90
		H14	2	2	H	H	S	K	D	K	I	D	G	W	L	T	Q	I	N	L	N	I	T
		H3	2302	1228	H	H	N	(N)/T (1)/1227	(N, Y,E,G)/D (35)/1193	(R,Q,M,N)/K (13)/1215	(M)/(V/I) (149)/(70%/30%)	(N)/D (15)/1213	G	W	(F)/L (1)/1227	T	Q	(V,T,L)/I (5)/1223	(D,S,T,A)/N (22)/1206	(M)/L (1)/1227	(D)/N (1)/1227	(V,T,F)/I (19)/1209	(A)/T (7)/1221
	H7	H15	8	5	H	H	N	T	P	L	I	D	G	W	Y	T	Q	I	T	L	N	I	A
		H7	334	273	H	H	N	T	(S,R,P)/N (131)/142	L	(V)/I (41)232	(N)/D (57)/213	G	W	(H)/Y (1)/272	T	(P)/Q (2)/271	(V)/I (3)/270	T	L	N	I	(T)/A (35)/238
		H10	31	28	H	H	N	T	(E)/K (1)/27	L	V	(N,E)/D (2)/26	(A)/G (1)/27	w	Y	T	Q	I	T	L	N	(V)/I (1)/27	A
# total sequences			6360	4178																			
Rate of non-conservative substitution at positions of major contact residue for both Groups.						2.18% **	2.15% **				0.17% ***	8.70%	0.00%	0.00%	0.05% ****	0.00%	0.00%	4.14%					

This table represents sequences available in public influenza sequence databases (http://www.ncbi.nlm.nih.gov/genomes/FLU/FLU.html) as of April. 17, 2008. Light blue highlights: top '( )/ ', (amino acid variant(s)) / amino acid consensus at the position; bottom '( )/ ', (number of amino acid variants)/ number of consensus amino acids. Non-highlighted amino acids are ~100% conserved or variants are observed ≤ 5 times at those positions for subtypes H4, H6, H9, H10, H11. Histidines H17 (HA1) and H111 (HA2) are buried and may play a role in pH-trigger are highlighted in green. ** H and Q are considered as conserved residues at these positions. *** V and I are both considered as conserved residues. **** Conserved residues include K, R and Q.

Supplementary Notes

Note S1. Epitope conservation and broad neutralization

We analyzed the location of the F10 epitopes in the fusogenic state, using the most complete model of the HA2 triple-helical conformation[2]. The reorganization to form the fusogenic state creates two major features that block access to the epitope observed in the neutral pH structure. First, one face of the αA helix involved in nAb binding becomes buried in the hydrophobic core of the new trimeric helical bundle (comprising residues 37_2-105_2 in H3). A second face of the helix is not obscured by the triple helix; instead it becomes inaccessible by virtue of the packing of a long C-terminal arm ("C-arm") of HA2, the last 23 residues of which form an extended conformation that packs tightly (and anti-parallel) against 2 helices, from residue 76_2 to 38_2.

Thus, considering the F10 epitope residues in αA, Lys 38 is partly-exposed at the base of the new trimeric helix, but makes H-bonds to the C-arm. Thr41 becomes fully buried within the helical trimer, and stabilizes the N-cap of its own helix via its hydroxyl side-chain, while its methyl side-chain combines with its symmetry mates to make the first annulus of the new hydrophobic core. Gln42 remains on the outer surface of trimer, but its side-chain makes H-bonds to two main-chain elements of the C-arm (171 C=O and 173 N), so it is fully obscured. It also stabilizes the conformation of Asp46 (H-bond) which salt-bridges to Arg170 from the C-arm. Ile45 becomes fully buried in the new trimeric core, and together with the preceding Ala44 forms a 6-membered hydrophobic annulus above the Thr41 annulus. Thr49 is exposed on the trimer surface, but makes an H-bond to 169 C=O and a hydrophobic contact with Leu168 (in H3, residues 49 is Asn, which is complemented by a change at position 168, also to Asn, with which it makes a bifurcated H-bond). In the Group 1 viruses, this is the only position with a significant change - Thr49Gln in H12. Simple modeling suggests that there is sufficient space for its side-chains to form H-bonds with 168 and 169 main-chain carbonyls, and also to complement a change at position 47 (Gly47Asn). Val52 becomes completely buried, and forms the next 3-membered annulus of the

hydrophobic core. Asn53 remains exposed on the helical surface, but its side-chain makes H-bonds to both the amide and C=O of residue 168. Finally, Ile56 becomes partly buried, contributing to the next hydrophobic (6-member) annulus with Ile55, and also packing tightly against the C-arm.

```
        38 41  45  49 52  56
         •  •   •   •  •   •
H2   ADKESTQKAVDGITNKVNSIIDK
H5   ADKESTQKAIDGITNKVNSIIDK
H1   ADQKSTQNAIDGITNKVNSVIEK
H6   ADRESTQKAVDGITNKVNSIIDK

H13  ADKESTQKAIDQITTKINNIIDK
H16  ADKTSTQKAINEITTKINNIIEK
H11  ADKESTQKAIDQITSKVNNIVDR

H8   ADQKSTQEAIDKITNKVNNIVDK
H12  ADRDSTQRAIDNMQNKLNNVIDK
H9   ADRDSTQKAIDKITSKVNNIVDK
-------------------------
H3   ADLKSTQAAIDQINGKLNRVIEK
```

We next examined all of the publicly available sequences (Supplementary Table 2). There are 2552 unique sequences for Group 1. When all sequences are considered, exceptions to the consensus are nearly always conservative, and if not very rare (< 0.1%). Of note, H5 is one of the most conserved, with an average of only 2.9 polymorphisms per residue (0.25%) with significant binding energy to F10 (from a data base of 1178 unique sequences). On this basis, and given the variety of CDR sequences in our Ab panel, we believe it reasonable to speculate, pending further data, that our Ab panel will neutralize the majority if not all of the Group 1 subtypes and their polymorphisms. The important point here though is that for those subtypes that are recalcitrant to our current Ab panel, we can simply apply our method to generate a new panel, and assemble a suitable cocktail.

Note S2. Murine mAb C179 neutralization spectrum. As discussed in the main text, C179 neutralized H1N1, H2N2, H5N3 and H5N9 of Group 1 viruses[3,4]. However it did not neutralize an H6 subtype[3]. The commercial vendor of C179 (Takara Bio USA) also provided additional information that it neutralized H9, but not H11 subtypes.

Note S3. Ref. 46 cited in the manuscript. From Table 1 of this reference (Kashyap, A. K. et al. Proc Natl Acad Sci U S A 2008, 105: 5986-91) we can deduce, based on the IMGT database (http://imgt.cines.fr/), that the VH germline gene used by these nAbs is VH1-69, previously designated as VH1e as reported.

Note S4. A recent report (Wrammert J. et al, Nature, 2008 453:667) sheds new light on this question. Data in this paper indicates that the humoral immune response against influenza virus is characterized by a highly restricted B-cell receptor repertoire in nature, and that more than half of the HA-specific human antibodies identified from antibody secreting cells (ASC) of influenza-vaccinated humans are raised against the globular head of HA (HA1) (This latter conclusion was not explicitly stated by the authors, but can be deduced from the data). Their data show that half of the HA-specific Abs are HI (hemagglutination inhibition) positive. Since some portion of HI-negative Abs are also HA1 specific, we can conclude that more than half of the HA-specific Abs are against HA1. The HA1 globular head is well-exposed and could be readily recognized by B cell receptors, and immune responses to this region are dominant in the vaccination procedure or by natural infection. Yet most if not all antibodies induced by this region lack cross-neutralizing-activity, owing to the great variability of HA1. Meanwhile, for conserved epitopes like the F10 epitope identified in our study, there may be a paucity of opportunities for B-cells to engage the epitope, and thus the host fails to mount a timely and productive neutralizing antibody response; or the Ab response against the F10-like epitope may be precluded due to other unknown mechanism(s).

Note S5. nAbs D8, F10 and A66 lack of autoreactivity. The three nAbs were tested for binding to self-antigens using standard clinical assays. The results show that the three nAbs do not bind to the following self-antigens: dsDNA, histone, Sm/RNP, SS-A, SS-B, Scl-70, centromere, PCNA, Jo-1, mitochondria, ribosomal-P protein, 60KD SS-A/Ro, Hep-2 cell extracts as well as cardiolipin. The highest antibody concentration tested in these assays is 100-200 μg mL^{-1}. Assays were performed using ELISA for detecting anti-nuclear antibodies (ANA) (QUANTA lite™ ANA ELISA kit, INOVA Diagnostics, Inc), ELISA for detecting anti-cardiolipin antibody (RELISA cardiolipin IgG kit, ImmunoConcepts Inc.) and HEP-2000 cell immunoflurecence (ImmunoConcepts Inc.).

Note S6. Small molecule inhibitors. Several small molecule inhibitors have been shown to neutralize influenza virus by inhibiting membrane fusion, although they lack broad cross-subtype neutralization, and are prone to immune escape. Russell et al.[5] have recently demonstrated crystallographically that a small molecule inhibitor of membrane fusion (specific to the Group 2, H3 cluster), TBHQ, binds in a cavity behind the “pocket” that is present in Group 2 but not Group 1 viruses[5]. In addition, an inhibitor of Group 1 viruses (H1 and H2 subtypes), BMY-27709, also acts by blocking membrane fusion, and its binding site has been tentatively mapped to $Phe110_2$, based on the ability of a Phe-Ser mutant to escape inhibition[6]. It may act by interfering with the $His111_2$-mediated pH trigger that is present in Group 1 but not Group 2 viruses. Most such inhibitors neutralize viruses with an IC_{50} in the μM range. *In vivo* efficacy data for these inhibitors are also currently lacking.

Supplementary Materials and Methods

Viruses, cells, HA and NA expressing plasmids. Wild type influenza A/Vietnam/1203/2004 (H5N1; H5-VN04), A/HongKong/483/1997 (H5N1; H5-HK97), A/Netherlands/219/2003 (H7N7; H7-NL03), , A/WSN/N/1933 (H1N1, H1-WSN33) and A/Ohio/4/1983 (H1N1; H1-OH83) viruses as well as a cold-adapted vaccine strain of A/Ann Arbor/6/1960 (H2N2; H2-AA60) , A/Sydney/5/97 (H3N2; H3-SY97), A/quail/Hong Kong/1721-30/99 (H6N1, H6-HK99), A/Chicken/New York/14677-13/1998 (H6N2; H6-NY98), H7-FP34 (A/FPV/Rostock/34 (H7N1)), A/turkey/Onatario/6118/68(H8N4; H8-ON68), A/chicken/HongKong/G9/97 (H9N2; H9-HK(G9)97), A/HongKong/1073/99 (H9N2, H9-HK99) were obtained from the WHO Global Influenza Surveillance Network and provided by Alexander Klimov (CDC, Atlanta, USA). A/Puerto Rico/8/1943 (H1N1; H1-PR34), Madin-Darby canine kidney (MDCK), Hela and 293T cells were obtained from the American Type Culture Collection and propagated in Dulbecco's Modification of Eagle's Medium with 10% fetal bovine serum. Viral infectivity was determined by plaque assay on MDCK cells. Live wild-type H5N1 viruses were handled in biosafety level 3 containment, including enhancements required by the U.S. Department of Agriculture and the Select Agents program http://www.cdc.gov/od/ohs/biosfty/bmbl5/bmbl5toc.htm. The full length HA gene (H5-TH04) of A/Thailand/2(SP-33)/2004 (H5N1) and neuramidase gene (N1) of H5-VN04 (Genbank accession AAW80723) were codon-optimized for eukaryotic cell expression and cloned into pcDNA3.1 vector to obtain the pcDNA3.1-H5-TH04 and pcDNA3.1-N1 expressing plasmids, separately. Full length HA subtypes including H1-WSN33, H2-AA60, , H6-NY98, H9-HK(G9)97, H9-HK99, H11(A/duck/Memphis/546/1974 (H11N9)), H13 (A/gull/Maryland/704/1977 (H13N6)) and H16 (A/shorebird/Delaware/172/2006 (H16N3)) were directly cloned from viral RNA and further subcloned into a pcDNA3.1 expression vector. See Acknowledgements for details on other subtype HAs.

HA1 is an N-terminal fragment of HA of H5N1 A/Thailand/2(SP-33)/2004 (H5-TH04), residues 11 to 325 (H3 numbering). The gene was codon-optimized for eukaryotic cell expression and expressed as fusion protein with a C-terminal 9 amino-acids tag (C9-tag: GTETSQVAPA). The fusion protein HA1-C9 was expressed in 293T cells transiently and the secreted proteins in supernatant were harvested 48 hours after transfection and purified from the supernatant by affinity chromatography using Protein A Sepharose that was coupled covalently with anti-C9 antibody 1D4 (National Cell Culture Center).

Expression and preparation of phage-scFvs, soluble scFv-Fcs and full-length human IgG1. Phage-scFvs of individual clones were produced as described previously[7]. scFv-Fcs and whole human IgG1 were produced as described previously[7-9]. In brief, selected scFvs were converted to scFv-Fcs by subcloning the scFv into an Fc expression vector pcDNA 3.1-Hinge, which

contains the hinge, CH2, and CH3 domains of human IgG1 but lacks CH1. For whole human IgG1s, the VH and VL gene fragments of scFv were separately subcloned into human IgG1 κ light chain or λ light chain expression vector TCAE5 or TCAE6[9]. scFv-Fcs or IgG1s were expressed in 293T or 293F cells (Invitrogen) by transient transfection and purified by protein A sepharose affinity chromatography.

ELISA. 0.2 μg of pure H5 HA proteins were coated onto 96-well Maxisorb ELISA plates (Nunc, NY) at 2 μg mL^{-1} in PBS at 4ºC overnight. The plates were washed 3 times with PBS to remove uncoated proteins. For regular ELISA, 1 μg mL^{-1} of anti-H5 scFv-Fcs followed by HRP-anti-human IgG1 were used to detect the binding of anti-H5 scFv-Fcs to H5 HA proteins. For competition ELISA, 50 μL(10^{12} pfu) of anti-H5 phage-scFvs were mixed with 5 μg mL^{-1} of anti-H5 scFv-Fcs and applied to H5-VN04 HA-coated ELISA plates. The competition of scFv-Fcs for the binding of phage-scFvs to HA0 was determined by measuring the remaining binding of phage-scFvs using HRP-anti-M13. The optical density at 450 nm was measured after incubation of the peroxidase tetramethylbenzidine (TMB) substrate system (KPL, Gaithersburg MD).

Haemagglutination inhibition (HI) assay. The HI assay was performed as previously described[10]. Briefly, H5N1/PR8[11], H5-VN04 and H1-PR34 viruses were mixed with log_2 antibody dilutions in PBS, and incubated at 20-22ºC for 30 min. A 0.5% suspension of turkey erythrocytes was added to each well, and the mixture incubated for 30 min at RT before visual scoring for haemagglutination activity.

Binding of anti-HA5 antibodies with H5-TH04 mutants. All mutants of pcDNA3.1-H5-TH04 were constructed by the QuikChange method (Stratagene, La Jolla, CA). Various full-length wild type HA and HA mutants expressing plasmids of H1, H5 or H7 were transfected transiently into 293T cells. 24 h after transfection, cells were harvested for immunostaining. Anti-H5 or control mAb 80R[7] at 10 μg mL^{-1} or ferret anti-H5N1 serum at 1:300 dilution were incubated with transfected 293T cells at 4ºC for 1 h. Cells were then washed three times with PBS containing 0.5% BSA and 0.1% NaN_3. FITC-labeled goat anti-human IgG (Pierce Biotech., Rockford, IL) or FITC-labeled goat anti-ferret IgG (Bethyl, Montgomery, TX) were then added to cells and incubated for 30 mins at 4ºC. Cells were washed as above, and binding of antibodies to cells was analyzed using a Becton Dickinson FACScalibur with CellQuest software.

Neutralization assay with HA-pseudotyped viruses. We produced the single-round HIV luciferase reporter viruses pseudotyped with viral envelopes of H5-TH04, H1-SC1918, H1-PR34, H2-JP57, H6-NY98 or H11-MP74 (See Supplementary Materials) by co-transfection of 293T cells with 4 plasmids: HA-expressing plasmid, HIV packaging vector pCMVΔR 8.2 encoding HIV-1 Gag-Pol; transfer vector pHIV-Luc encoding the firefly luciferase reporter gene under

control of the HIV-1 LTR; and N1-expressing plasmid pcDNA3.1-N1. The ratio of H5- to N1-expressing plasmids was 4:1. After 8-12h transfection, the medium was changed to serum-containing medium (for H5) or serum-free DMEM medium supplemented with 0.2% (w/v) BSA (for H1, H2, H6 and H11). Viral supernatants were harvested at 36h post-transfection. Prior to neutralization tests, supernatants containing pseudotyped viruses (except H5N1) were incubated with 16 μg ml^{-1} TPCK-treated trypsin for 1h at 25°C, and then neutralized with trypsin-neutralizing solution (TNS, Cambrex) at a ratio of 1:1 (v/v). The neutralization assay was performed as previously described[12]. Viral entry level was evaluated by measuring luciferase activity in target cells.

Surface Plasmon Resonance (SPR) analysis. Kinetic analyses of H5 HA mAbs binding to recombinant H5-VN04 HA0 trimer were performed on a Biacore T100 (Biacore, Sweden) at 25ºC. Anti-human IgG Fc antibody (Biacore) was covalently attached to individual flow cell surfaces of a CM4 sensor chip by amine-coupling using the amine coupling kit (Biacore). HA mAbs were captured onto anti-human IgG Fc surfaces (flow rate of 10 μl min^{-1} in HBS buffer (Biacore)) to ensure that mAb-H5 binding occurred as a homogenous 1:1 Langmuir interaction. H5 HA was injected over each flow cell at a flow rate of 30 μl min^{-1} in HBS buffer, and at concentrations ranging from to 0.31 to 20 nM. A buffer injection served as a negative control. All experiments contained an additional anti-human IgG Fc antibody control surface that accounted for changes in the buffer refractive index and to test for potential nonspecific interactions between H5 HA and anti-human IgG Fc. Upon completion of each association and dissociation cycle, surfaces were regenerated with 3 M $MgCl_2$ solution. The association rates (*ka*), dissociation rates (*kd*), and affinity constants (K_D) were calculated using Biacore T100 evaluation software. The quality of each fit was based on the agreement between experimental data and the calculated fits, where the Chi^2 values were below 1.0. Surface densities of mAbs against H5 HA were optimized to minimize mass transfer and avoid any contribution of avidity effects. All *ka, kd,* K_D values reported here represent the mean and standard error of three experiments.

In vivo inhibition by nAbs of virus replication in lung, brain and spleen. Three human nAbs (D8-IgG1, F10-IgG1 and A66-IgG1) or control nAb 80R-IgG1 were administered at 15 mg kg^{-1} into groups of 10 mice by intraperitoneal (i.p.) injection in a volume of 0.5 mL 24h, 48h and 72h after inoculation with $10xMLD_{50}$ of H5-VN04 or H5-HK97 by the intranasal (i.n.) route. To determine viral titers in different organs of H5-VN04-infected mice, 5 animals in each group were euthanized at 4 days post-inoculation, and the lungs, brains, and spleens were aseptically removed and homogenized. Viral infectivity titers in homogenized tissue suspensions were determined by plaque assay on monolayers of MDCK cells. The viral titer is expressed as plaque-forming units per gram (pfu g^{-1}) of tissue. The remaining 5 mice were weighed and observed for 2 weeks after inoculation. Body weight was recorded daily for two weeks.

Expression and purification of F10 scFv and H5 for crystalization.

The gene encoding F10 scFv (VH-linker-VL) was cloned into a pSynI vector containing an N-terminal periplasmic secretion signal, pelB, and a C-terminal His_6 tag. F10 scFv was expressed in XL10 cells in 2YT media containing 0.1% glucose (w/v) at 25°C for 15h with 0.5 mM IPTG. Protein was purified first by Hisbind Ni-NTA (Novagen) according to the manufacturer's instructions, and then by Superdex 200 (Amersham Biosciences) in 50 mM Tris-HCl, 0.5 M NaCl, pH 8.

The ectodomain of H5-VN04 HA gene was expressed in insect cells as a fusion protein by adapting the protocol described previously[13]. This construct contains a C-terminal trimerizing 'foldon' sequence from the bacteriophage T4 fibritin to stabilize the trimeric structure, followed by a thrombin site and a His_6 tag. The cDNA of the fusion protein was cloned into the baculovirus transfer vector, pAcGP67A (BD Biosciences, Bedford, MA), to allow for efficient secretion of recombinant protein. To obtain fully cleaved HA (as HA1-HA2 trimers), sf9 cells were co-infected with baculovirus stocks of HA0 and furin at an empirically derived ratio. The furin cDNA was a gift from Dr. Robert Fuller (University of Michigan). Three days after infection, the cells were spun down and the supernatant was incubated with Ni-NTA beads (Qiagen Inc., Valencia, CA). The beads were washed with TBS buffer (10 mM Tris.HCl, 80 mM NaCl, pH 8.0) with 10 mM imidazole, and eluted with TBS with 250 mM Imidazole. The eluted H5 protein was dialyzed against TBS buffer and further purified by ion-exchange using Mono Q HR10/10 column (GE Healthcare, Piscataway, NJ). The purified H5 was digested by thrombin overnight and further purified by Superdex 200 column in TBS buffer.

Comparison of two trimers in asymmetric unit. The RMS differences between our refined H5 trimers in the F10 complex and the H5 starting model (2IBX) are 1.0 and 0.63 Å for all Cαs. The value for the second trimer is close to that expected on the basis of random error alone; the larger value for the first arises from a twist of the stem region with respect to the head by a few degrees about a vertical axis. When the two copies of the complex are superposed, the head regions overlay closely, but the stems diverge as a function of distance both from the head and from the 3-fold axis, such that the outer parts of the stem at the Ab interface shift by ~3 Å. However, this does not affect the antibody-antigen contacts, and 3-fold symmetry is maintained. These differences explain why 6-fold or 2-fold non-crystallographic symmetry (ncs) refinement was unsuccessful, although, in retrospect, we could have used 2x3-fold ncs with distinct masks for the two trimers. However, refinement without ncs converged successfully, utilizing the high resolution starting models fitted locally to the refined models after each round of automatic refinement as guides during model-building.

References

1. Chothia, C. et al. Structural repertoire of the human VH segments. *J Mol Biol* **227**, 799-817 (1992).
2. Chen, J., Skehel, J.J. & Wiley, D.C. N- and C-terminal residues combine in the fusion-pH influenza hemagglutinin HA(2) subunit to form an N cap that terminates the triple-stranded coiled coil. *Proc Natl Acad Sci U S A* **96**, 8967-72 (1999).
3. Smirnov, Y.A. et al. An epitope shared by the hemagglutinins of H1, H2, H5, and H6 subtypes of influenza A virus. *Acta Virol* **43**, 237-44 (1999).
4. Okuno, Y., Isegawa, Y., Sasao, F. & Ueda, S. A common neutralizing epitope conserved between the hemagglutinins of influenza A virus H1 and H2 strains. *J Virol* **67**, 2552-8 (1993).
5. Russell, R.J. et al. Structure of influenza hemagglutinin in complex with an inhibitor of membrane fusion. *Proc Natl Acad Sci U S A* (2008).
6. Luo, G. et al. Molecular mechanism underlying the action of a novel fusion inhibitor of influenza A virus. *J Virol* **71**, 4062-70 (1997).
7. Sui, J. et al. Potent neutralization of severe acute respiratory syndrome (SARS) coronavirus by a human mAb to S1 protein that blocks receptor association. *Proc Natl Acad Sci U S A* **101**, 2536-41 (2004).
8. Gould, L.H. et al. Protective and therapeutic capacity of human single-chain Fv-Fc fusion proteins against West Nile virus. *J Virol* **79**, 14606-13 (2005).
9. Reff, M.E. et al. Depletion of B cells in vivo by a chimeric mouse human monoclonal antibody to CD20. *Blood* **83**, 435-45 (1994).
10. Donald, H.B. & Isaacs, A. Counts of influenza virus particles. *J Gen Microbiol* **10**, 457-64 (1954).
11. Subbarao, K. et al. Evaluation of a genetically modified reassortant H5N1 influenza A virus vaccine candidate generated by plasmid-based reverse genetics. *Virology* **305**, 192-200 (2003).
12. Sui, J. et al. Evaluation of human monoclonal antibody 80R for immunoprophylaxis of severe acute respiratory syndrome by an animal study, epitope mapping, and analysis of spike variants. *J Virol* **79**, 5900-6 (2005).
13. Stevens, J. et al. Structure and receptor specificity of the hemagglutinin from an H5N1 influenza virus. *Science* **312**, 404-10 (2006).